Stimulus-Induced Relief of Intentionally Incorporated Frustration Drives Refolding of a Water-Soluble Biomimetic Foldamer

Hanne C. Henriksen[‡], Adam J. Sowers[‡], Christopher R. Travis[‡], Troy D. Vulpis[‡], Thomas A. Cope[‡], Sarah K. Ouslander[‡], Alexander F. Russell[‡], Michel R. Gagné[‡], Vojislava Pophristic[¶], Zhiwei Liu[¶], Marcey L. Waters*[‡]

KEYWORDS: Foldamers, frustration, frustrated interactions, switchable, non-covalent interactions, stimulus responsive

ABSTRACT: Frustrated, or nonoptimal, interactions have been proposed to be essential to a protein's ability to display responsive behavior, such as allostery, conformational signaling, and signal transduction. However, the intentional incorporation of frustrated noncovalent interactions has not been explored as a design element in the field of dynamic foldamers. Here we report the design, synthesis, characterization, and MD simulations of the first dynamic water-soluble foldamer that, in response to a stimulus, exploits relief of frustration in its noncovalent network to structurally rearrange from a pleated to intercalated columnar structure. Thus, relief of frustration provides the energetic driving force for structural rearrangement. This work represents a previously unexplored design element for development of stimulus-responsive systems that has potential application to materials chemistry, synthetic biology, and molecular machines.

INTRODUCTION

A critical aspect of many proteins is their ability to exhibit complex responsive behaviors such as allostery¹⁻³, conformational signaling⁴, and signal transduction^{5,6}, which often involves long-distance structural rearrangement. These responsive events must be transmitted through the noncovalent network (NCN) that makes up the tertiary structure of the protein. Wolynes and coworkers developed a theoretical model based on relief of frustration to describe how proteins respond to stimuli invoking long distance transmission, the key feature being nonoptimal, or frustrated, local noncovalent interactions (NCIs) within the globally stable protein structure. 7-11 Coupling of a stimulus, such as ligand binding or covalent modification, with relief of frustration can provide the energetic driving force required for long-distance structural changes. Indeed, computational studies have shown that dynamic regions of the protein that undergo conformational changes in response to a stimulus exhibit weaker interactions and more frustration than those within the core of the protein.⁷

Foldamers adopt well defined structures that provide the features necessary to recapitulate such complex behavior observed in proteins, providing an approach to create complex abiotic responsive systems. However, while dynamic foldamers that mimic allostery^{12–15} and stimulus response^{12,16–24} have been reported^{25–30}, to the best of our knowledge, relief of frustration has

not been used as a design element to induce long-distance structural reorganization in abiotic systems to date. Currently, the only reported example suggesting frustration as the driving force for structural rearrangement is a self-assembled [2]-catenane mutational study from our group³¹, however, frustration was not intentionally incorporated in the system design as a mechanism for complex behavior. Herein, we are the first to report the design and evaluation of a novel water-soluble foldamer in which we intentionally incorporate frustration coupled with a stimulus-responsive element to induce long-distance structural reorganization. Using UV-Vis, NMR, and molecular dynamics (MD) simulations, we demonstrate that the introduction of a stimulus weakens a favorable NCI allowing for the relief of a frustrated NCI, together changing the balance of powers within the NCN and driving the adoption of a new folded state. Thus, the frustrated interactions may be considered a source of latent free energy that is mechanistically linked to the stimulus.31 This work demonstrates frustration as a successful design principle and represents a first step in incorporating frustration as an intentional element in responsive foldamers, ultimately increasing the toolkit for the construction of complex supramolecular systems with potential applications to materials chemistry, molecular machines, and synthetic biology.

[‡]Department of Chemistry, CB 3290, UNC Chapel Hill, Chapel Hill, NC 27599 USA

Department of Chemistry and Biochemistry, Rowan University, Glassboro, NJ 08028-1701 USA

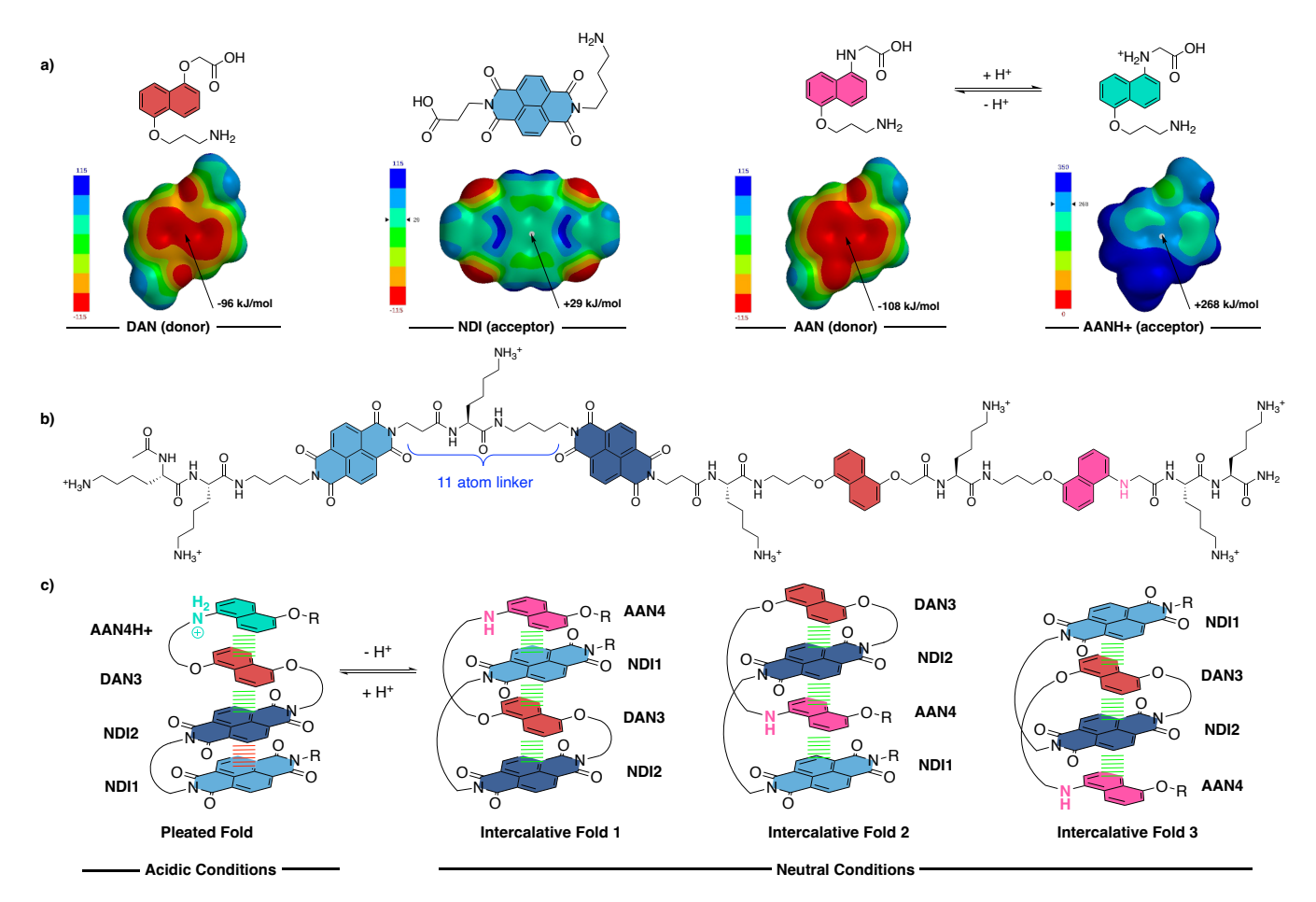


Figure 1. (a) Structure of DAN, NDI, AAN and AANH+ with their associated electrostatic potential maps (ESPs). ESPs of DAN, NDI, and AAN are scaled from -115 to +115 kJ/mol, AANH+ is scaled 0 to +350 kJ/mol. ESPs were calculated using gas phase DFT B3LYP 6-31G* with methyl groups in place of the sidechains (b) Structure of ADAM with AAN shown under neutral conditions (c) Cartoon representation of ADAM showing the major predicted pleated stacking orientation under acidic conditions and the major pseudo-degenerate intercalated stacking orientations under neutral conditions. Green dashed lines indicate optimized interactions and red dashed lines indicate frustrated interactions.

RESULTS AND DISCUSSION

System Design. The design of a stimulus-responsive foldamer with the potential to access two different folded states via the relief of frustration, requires the following elements: (1) a high degree of flexibility, (2) a site that will react with a stimulus, and (3) intentional frustration in one state that can be relieved in the second state in response to a stimulus. Additionally, to increase biomimetic relevance, we wanted the foldamer to function in aqueous solution. To accommodate these criteria, our foldamer design was adapted from Iverson's aromatic electron donor-acceptor foldamer,³² modified to incorporate a stimulus responsive element and a frustrated site, which we call the Adaptive Donor-Acceptor Motif (ADAM, Figure 1). Iverson's well-characterized system consists of π - π stacking interactions between alternating 1,5-dialkoxynaphthalene (DAN) and naphthalene diimide (NDI) monomer units connected with flexible peptidic linkers (Figure 1), and has been shown to fold in an aqueous environment.33,34

Furthermore, Iverson has shown that in a 3-subunit foldamer, the 11-atom linkers allow for folding into either a pleated or intercalative structure, depending on the ordering of NDI and DAN. In the pleated structure all stacking interactions are

formed via adjacent monomers, while the intercalative structure is formed via the stacking of nonadjacent monomers.35 While Iverson's system provides an established backbone structure, it was designed to exhibit only favorable donor-acceptor interactions. We chose to introduce protonation as the switch in the initial design of the frustrated foldamer by incorporating a novel aromatic subunit, aminoalkoxynaphthalene (AAN), an adaptation of DAN in which one of the naphthyl alkoxy groups is replaced with an amine. Protonation of the naphthylamine to AANH+ reverses the electrostatics from an electron-rich donor to an electron-poor acceptor (Figure 1a). We expected that this would result in a change in its stacking preference: at acidic pH, AANH+ is electron deficient and is expected to prefer stacking with DAN. Upon deprotonation, AAN becomes electron rich and thus should prefer stacking with NDI over DAN. We envisioned exploiting this change in stacking preference by mechanistically coupling it with the relief of frustration to drive a structural rearrangement.

The sequence of the ADAM foldamer, NDI1-NDI2-DAN3-AAN4 from N- to C-terminus with a lysine residue linking each aromatic subunit for water solubility, was designed to incorporate frustration in both acidic and neutral conditions (Figure 1b). In an acidic environment where AAN4H+ is electron poor and expected to stack with DAN3, NDI1 lacks an electron-rich

partner and thus is predicted to stack with NDI2 to minimize exposed surface area.36 pleated solvent Α NDI1•NDI2•DAN3•AAN4H+ structure (where • indicates a stacking interaction; Figure 1c, left) is the expected minimum energy structure. This represents a frustrated situation as NDI•NDI stacking has been shown to be approximately 10-fold weaker than NDI•DAN stacking.³⁷ At neutral pH, when AAN is not protonated and thus electron rich, we hypothesized it would weaken the interaction with DAN3 and trigger a stimulus-response in which AAN would induce long distance communication through the NCN by favoring an AAN•NDI stack that relieves the NDI1 NDI2 frustration. Three possible intercalative folds achieve this (Figure 1c, right): NDI1 can swing up to insert between DAN3 and AAN4 (intercalative fold 1), AAN4 can swing down to insert between NDI1 and NDI2 (intercalative fold 2), or NDI1 can swing up to stack with DAN3 and AAN4 can swing down to stack with NDI2 (intercalative fold 3). Thus, the ADAM foldamer demonstrates a second principle of protein function, that of conformational dynamics, 38,39 since the requirement for a flexible foldamer results in several pseudo-degenerate low-energy structures at neutral pH. These intercalative stacks maintain the minimized solvent-exposed surface area as well as the core NDI2•DAN3 stack while maximizing donor-acceptor interactions. In these states, we expect that frustration arises from the entropic cost of the intercalative stacking in which the linkers have less entropic freedom. Thus, going in the reverse direction from the neutral to protonated state, the AANH+•NDI interactions will be unfavorable, driving the foldamer back to the pleated structure.

Synthesis. Subunits AAN, DAN, and NDI were synthesized as Alloc-protected amino acid derivatives for solid phase peptide synthesis using modifications of literature procedures for DAN and NDI (see SI) and the approach shown in Scheme 1 for Alloc-AAN-OH.^{32,33} Initial attempts to synthesize them as Fmocprotected amino acids resulted in poor solubility and thus poor peptide incorporation. The ADAM foldamer and a series of control peptides (Table 1) were synthesized by solid-phase peptide synthesis (see SI).

Scheme 1. Synthetic route of novel monomer Alloc-AAN-OH.

Table 1. Peptide sequences and their associated abbreviations^a

Abbreviation	Peptide Sequence	
NDI monomer	Ac-K-NDI-K-NH ₂	
DAN monomer	Ac-K-DAN-K-NH ₂	
AAN monomer	Ac-K-AAN-K-NH ₂	
NDI-AAN	Ac-K-NDI-K-AAN-K-NH2	
NDI-DAN	Ac-K-NDI-K-DAN-K-NH ₂	
NDI-NDI	Ac-K-NDI-K-NDI-K-NH ₂	
DAN-AAN	Ac-K-DAN-K-AAN-K-NH2	
ADAM	$Ac\text{-}K\text{-}K\text{-}NDI\text{-}K\text{-}DAN\text{-}K\text{-}AAN\text{-}K\text{-}K\text{-}NH_2$	

(a) Lysine is represented by the letter K. Ac represents an acetyl cap at the N-terminus. $-NH_2$ indicates that the C-terminus is an amide. One additional lysine residue at each terminus was incorporated in ADAM to increase water solubility.

pH Dependence, UV-Vis and ¹H NMR Spectra of AAN, DAN, and NDI Monomer Peptides. To determine the pH at which AAN becomes protonated, we measured the UV-Vis spectrum of the AAN monomer peptide at various pHs. Protonation of the naphthyl amine results in a characteristic blue shift in the UV spectrum at pH 0 (Figure S20c), while no blue shift is observed at pH 3. This is consistent with the literature pKa of a similar amino acid, N-phenylglycine methyl ester (pKa 2.0).⁴⁰ Based on this, all studies at neutral pH were performed in 50 mM sodium phosphate D₂O buffer (pD 7, uncorrected), while acidic studies were conducted in 1 M D₂SO₄ in D₂O (pD 0, uncorrected). We also verified that the DAN and NDI monomer UV-Vis spectra are independent of pH, indicating that they do not become protonated in this pH range (Figure S20a-b).

¹H NMR studies further corroborated the pH-dependent protonation of AAN and pH independence of DAN and NDI monomer peptides, as peak shifting was observed for the AAN monomer peptide when comparing the spectra at neutral and acidic conditions, but not for the NDI or DAN monomer peptides (Figure S22). This verifies that AAN is the only monomer protonated under acidic conditions and can behave as the sole pH switch in the ADAM foldamer.

Dimer Peptide Control Studies. UV-Vis and 1H NMR studies were also used to confirm stacking and folding of the NDI-DAN, NDI-AAN, and NDI-NDI dimer peptides under both conditions as simpler models for the ADAM foldamer. UV-Vis analysis of the NDI-DAN dimer peptide confirmed the literature-precedented charge transfer (CT) complex between NDI and DAN, 32 appearing red in solution with a λ_{max} at 514 nm in both neutral and acidic solutions (Figure S21a). This supports NDI-DAN stacking in both conditions. The NDI-AAN peptide in neutral conditions exhibits a distinct CT band with a λ_{max} at 613 nm, resulting in a visible green color, also indicating stacking (Figure S21c). This CT band is lost upon protonation of AAN under acidic conditions, as protonated AANH+ cannot act as a donor for charge transfer. No other dimer peptides produced a CT band in either solution.

We observed upfield shifting of the 1H NMR aromatic region of NDI-NDI, NDI-DAN, NDI-AAN and DAN-AAN dimer peptides in both neutral and acidic solution relative to their respective monomer peptides, as well as splitting of the NDI singlet peak. This is expected for π - π stacking interactions and further supports folding in all dimer systems (Figure S23). Additionally, the dimer spectra for NDI-NDI and NDI-DAN are

identical at both conditions, further demonstrating that NDI and DAN are pH independent when stacked. In contrast, the ¹H NMR spectra for NDI-AAN and DAN-AAN dimers show differences in chemical shifts between the spectra under acidic and neutral conditions, supporting the conclusion that AAN is required for pH-dependent changes. In summary, only AAN demonstrated pH dependent behavior. Information from the dimer peptides was used as a template to interpret the more complex data from our ADAM foldamer.

Characterization of ADAM at pH 0. Dilution studies of ADAM were performed in both acidic and neutral solution to confirm the absence of aggregation. Using the Beer-Lambert equation, we confirmed that absorbance and concentration of ADAM are linearly correlated between 100 µM and 2 mM (Figure S43), suggesting aggregation is not present within this concentration range.

UV-Vis of ADAM in acidic solution confirms that ADAM contains a DAN•NDI stack, as indicated by the red CT band at 514 nm (Figure 2a). However, since AANH+ cannot form a CT complex in its protonated state, UV-Vis does not report on its interaction.

We undertook NMR experiments, including variable temperature ¹H NMR and NOESY experiments, to characterize the folded state and provide insight into the stacking interactions. The ¹H NMR spectrum exhibits upfield shifting of all aromatic peaks relative to the monomer peptides, demonstrating extensive stacking of all residues. However, at 298 K, all peaks are broadened, indicating intermediate exchange rates. Heating to 318 K results in significant sharpening with only minimal changes in chemical shift indicating an increase in exchange rates without disrupting stacking interactions.

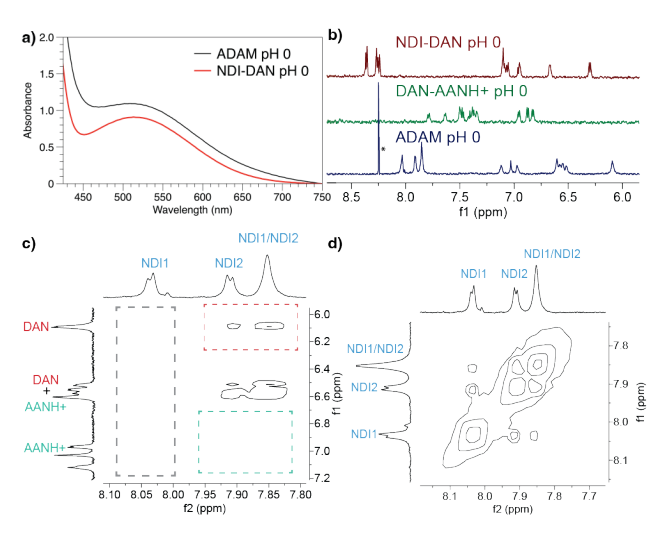


Figure 2. (a) CT bands for NDI-DAN and ADAM under acidic conditions (b) Stacked ¹H NMR of NDI-DAN, DAN-AANH+, and ADAM peptides in pD 0 solution at 298 K for NDI-DAN and DAN-AANH+ and 318 K for ADAM; * indicates impurity. (c) ADAM pD 0 2D NOESY spectrum highlighting crosspeaks between one of the NDIs and the DAN peak at 6.09 ppm, and the lack of crosspeaks between NDI and AANH+ (d) ADAM pD 0 2D NOESY NMR highlighting crosspeaks between both NDIs. ADAM concentrations are ~1 mM for UV-Vis and 2 mM NMR respectively. Dimer concentrations are 100 uM for NMR.

The NOESY spectrum at 318 K exhibits crosspeaks between the most upfield aromatic peak at 6.09 ppm, corresponding to DAN and only one of the two NDIs (Figure 2b,c). This is consistent with DAN•NDI stacking that results in the red CT band observed in the UV-Vis spectrum. In contrast, the aromatic peak at 6.97 ppm, which corresponds to AANH+, does not exhibit NOEs to any of the NDI peaks, consistent with the expected pleated columnar fold in which AANH+ is distal from both NDIs. Because of the overlap of DAN and AANH+ crosspeaks between 6.50 - 6.62 ppm, we cannot determine whether there are any NOEs between DAN and AANH+. Furthermore, the most downfield NDI peak at 8.03 ppm does not exhibit crosspeaks to DAN or AAN, but does exhibit NOEs to the other NDI peaks (Figure 2d), consistent with the designed frustrated NDI•NDI stack, suggesting it is the terminal NDI1. Combined, these data support the pleated columnar folded state shown in Figure 1c (left), in which the aromatic residues NDI1•NDI2•DAN3•AAN4H+ stack in the order that they are linked.

Characterization of ADAM at pH 7. To characterize the donor-acceptor stacking interactions in ADAM under neutral conditions, we compared its UV-Vis spectrum to those of the NDI-DAN and NDI-AAN dimer peptides (Fig. 3a). The UV-Vis spectrum of ADAM exhibits a distinct CT band with a λ_{max} at 540 nm, corresponding to a black color in solution. This CT band has the same λ_{max} as the sum of the CT bands for NDI-DAN and NDI-AAN, indicating that both DAN3 and AAN4 stack with NDI at neutral pH.

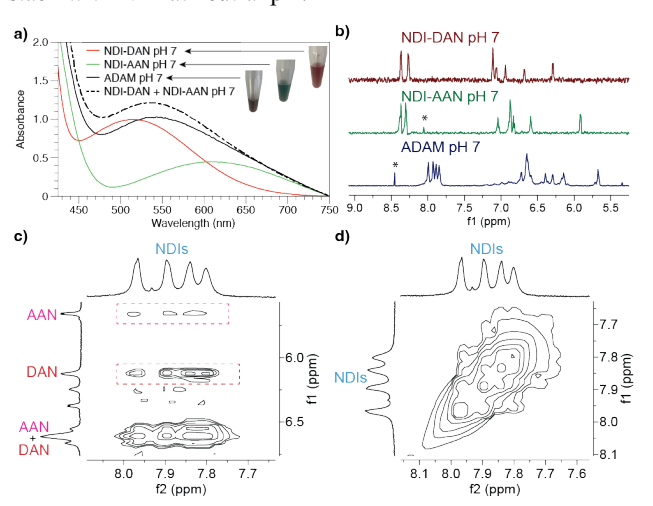


Figure 3. (a) CT bands for NDI-DAN, NDI-AAN, NDI-DAN+NDI-AAN and ADAM under neutral conditions, as well as photos of NDI-DAN, NDI-AAN, and ADAM solutions. (b) Stacked ¹H NMR of NDI-DAN, NDI-AAN, and ADAM peptides in pD 7 solution at 298 K for NDI-DAN and NDI-AAN and 318 K for ADAM; * indicates impurity. (c) ADAM pD 7 2D NOESY spectrum highlighting crosspeaks between both NDIs and DAN and AAN peaks (d) ADAM pD 7 2D NOESY NMR highlighting crosspeaks between the aromatic NDIs. ADAM concentrations are ~1 mM for UV-Vis and 2 mM NMR respectively. Dimer concentrations are 100 uM for NMR.

Analysis of the NOESY at neutral pH further supports the assertion that both AAN and DAN interact with both NDIs (Figure 3c). The DAN peak at 6.13 ppm exhibits NOEs to both NDIs, supporting NDI1 intercalation. The AAN proton at 5.67 ppm exhibits NOE crosspeaks to both NDIs, also suggesting intercalated stacking of AAN4. These results are both consistent with the observed CT spectrum that indicates both the AAN•NDI and DAN•NDI stacks are present, as expected in the

intercalated columnar structures. The NOESY crosspeaks of DAN and AAN to both NDIs are consistent with a conformational ensemble of more than one of the pseudo-degenerate stacked structures. Additionally, the NOESY spectrum shows crosspeaks between the two NDIs, suggesting some degree of NDI1•NDI2 stacking (Figure 3d).

Molecular Dynamics (MD) Simulations. To gain insight into the conformational preferences of the foldamer, we performed MD simulations on the protonated and neutral ADAM foldamers in explicit water. Multiple starting structures and a simulated annealing scheme were used to ensure sufficient conformational sampling. The partial atomic charges of the aromatic units were obtained by a multi-conformational RESP charge derivation method.41 To analyze the aromatic stacking within the foldamer, we calculated the distance between the center of masses of two aromatic ring systems for all the possible pairs of aromatics, as well as the angles between the two aromatic planes for all structures in the MD trajectories. We then examined the distribution of distances and angles as a function of simulation time and as an ensemble collective using histograms. We observed distance distribution having peaks around 3 to 4 Å and angle distribution having peaks around 5 to 10 degrees. Both agree well with aromatic stacking; therefore, a combined distance (< 5.5 Å) and angle (< 25°) criterion was set based on the distribution data. The aromatic stacking pattern was then determined by applying the criterion to all the aromatic pairs.

Analysis of the pairwise stacking over all MD trajectories (Table 2) under acidic conditions indicates that the predicted NDI1•NDI2 frustrated stack and NDI2•DAN3 stack are present in the majority of structures, 80% and 75%, respectively. However, the predicted stacking of DAN3•AAN4H+ is lower than expected at only 21%. Other interactions suggest a small degree of misfolding, consistent with the flexible nature of this foldamer, allowing for conformational dynamics.

Table 2. Statistics of stacking. Percentage of stacking is calculated based on MD trajectories totaling to 2800 ns at 300K for each sequence.

Stacking Pair	At acidic pH	At neutral pH
NDI1•NDI2	80%	27%
NDI2•DAN3	75%	78%
DAN3•AAN4H+/AAN	21%	2%
NDI1•AAN4H+/AAN	6%	68%
NDI2•AAN4H+/AAN	25%	39%
NDI1•DAN3	25%	50%

Additional insight comes from analysis of the probabilities of different folded conformations in acidic conditions (Figure 4). At acidic pH, 58% of the time, the foldamer has the expected NDI1•NDI2•DAN3 stack, with 18% also containing the DAN•AAN4H+ stack, and 40% with AAN4H+ frayed (Figure 4a). This preference for AAN4H+ to swing away from the stacked system at the terminus explains why DAN3•AAN4H+ has a lower predicted stacked percentage at just 21% (Table 2). However, upfield shifting of AAN4H+ aromatic peaks relative to the AAN4H+ monomer peptide suggests that it may be more significantly stacked than indicated in the MD simulations (Figure S25). Additionally, 7% contain an NDI2-NDI1-DAN stack,

in which the order of NDIs is reversed, again with fraying of AAN4H+ (Figure 4b). Taken together, 65% of the protonated computational structures adopt the designed pleated structure (Figure 1c, left). The experimental data also revealed more variability with respect to the order of NDI1 and NDI2 and more fraying of AAN4H+ than was expected, attributable to conformational dynamics. An additional ~13% of the protonated foldamer "misfolds" into an NDI1 DAN3 NDI2 intercalative stack, which lacks the frustrated NDI•NDI interaction, but has the addition of a frustrated NDI•AAN4H+ interaction (Figure 4c). However, the lack of NDI-AANH+ NOEs indicates some divergence between the MD simulations and experimental data. Furthermore, ~10% of the protonated foldamer is a misfolded NDI1•NDI2•AAN4H⁺•DAN3 stack which contains both NDI1•NDI2 and NDI•AAN4H+ frustrated interactions (Figure 4d); this orientation is likewise not supported by experimental NMR spectra.

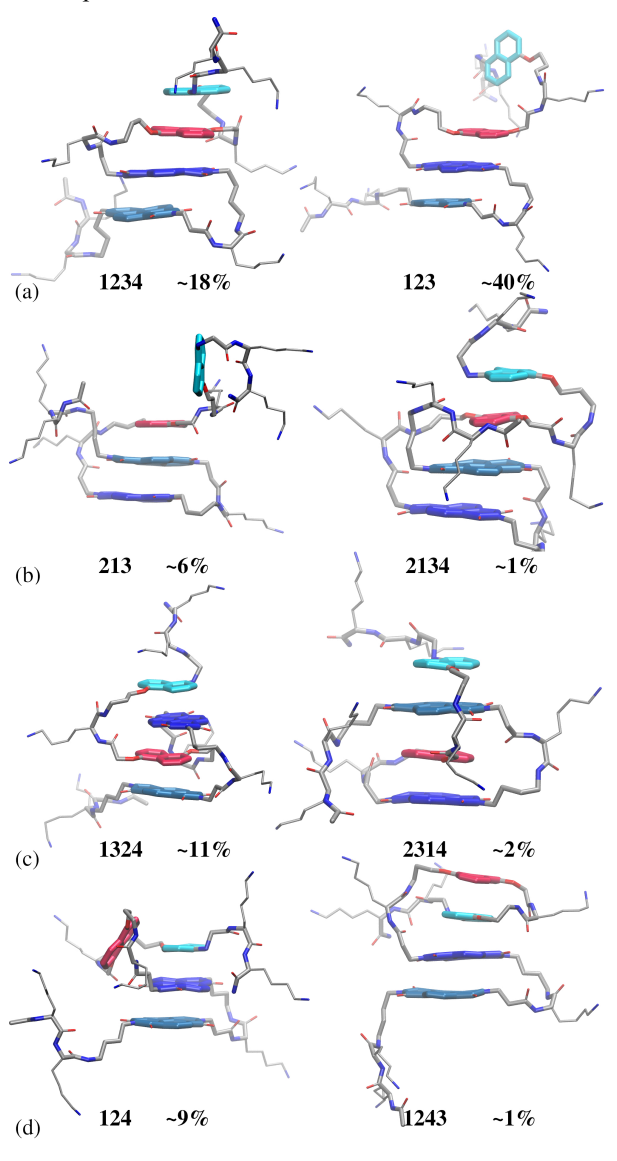


Figure 4. MD simulations of ADAM in the protonated state. Numbers indicate the order in which the four aromatic groups stack; percents indicate the probabilities that ADAM adopts a particular folded structure. (a) Major conformations that are consistent with the system design. (b) Conformations where the expected interactions are present but NDI1 and NDI2 are reversed. (c) "Misfolded" conformations with intercalative stacking of DAN between NDI1

and NDI2 and a frustrated NDI-AANH+ interaction. (d) "Misfolded" conformations with a frustrated NDI-AANH+ interaction.

Under neutral conditions, analysis of the pairwise stacking over all MD trajectories (Table 2) indicates a significant decrease in the percent stacking for NDI1•NDI2, dropping from 80% stacked at acidic pH to 27% stacked at neutral pH, suggesting a change in folding with a relief of the NDI•NDI frustration. Additionally, there is a 10-fold decrease in stacking between DAN3 and AAN4 (from 21% to 2%), an 11-fold increase in NDI1•AAN4 stacking (from 6% to 68%), and a two-fold increase in NDI1•DAN3 percent stacked (from 25% to 50%), consistent with intercalative stacking. This, coupled with the retention of the core NDI2•DAN3 stack at 78%, supports the experimental evidence that a long-distance structural reorganization takes place with a change in pH.

Analysis of the distribution of conformers under neutral conditions (Figure 5) indicates that the three major species all represent intercalated folds (Figure 1c): NDI2•DAN3•NDI1•AAN4 (32%, fold 1), NDI1•AAN4•NDI2•DAN3 (17%, fold 2), and NDI1•DAN3•NDI2•AAN4 (11%, fold 3). These folded structures are pseudo-degenerate in terms of the number of donoracceptor interactions and the number of non-adjacent stacking interactions. In each, the adjacent stacking of NDI2 and DAN3 is maintained. All three structures are consistent with the observed NOEs and CT data. An additional 3% is in an extended sheet-like conformation with greater solvent-exposed surface area (Figure 5a).

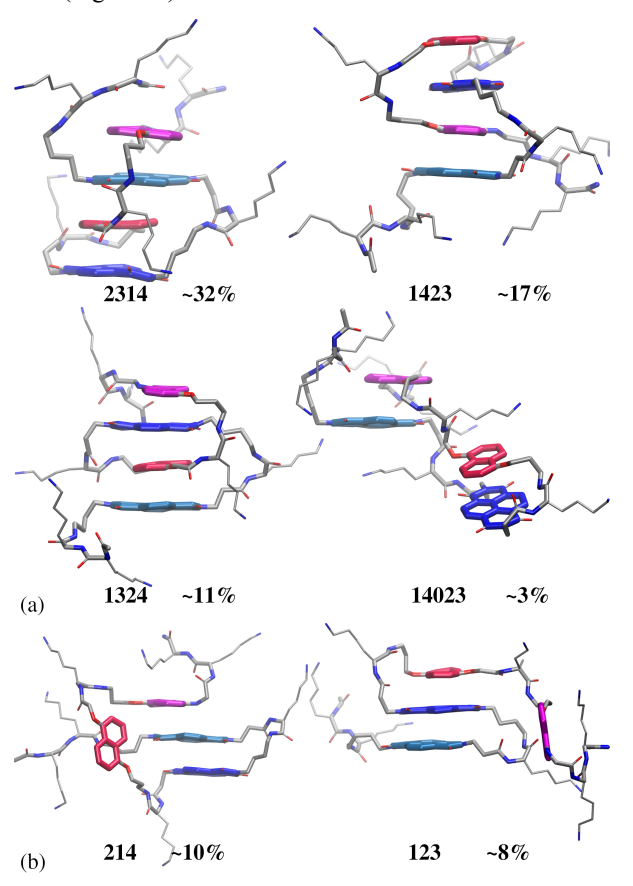


Figure 5. MD simulations of ADAM in the neutral state. Numbers indicate the order in which the four aromatic groups stack; percents indicate the probabilities that ADAM adopts a particular folded structure. (a) Major conformations that are consistent with the

system design. (b) "Misfolded" conformations maintaining the NDI-NDI stack.

Some minor species are also consistent with the observed experimental NDI1•NDI2 NOEs at neutral pH. An NDI1•NDI2•AAN4 stack with DAN3 outside of the stack accounts for 10% of the computational structures, while 8% was found to be in a misfolded NDI1•NDI2•DAN3 stack with AAN frayed, (Figure 5b). All other species were ≤ 4% of the total structural data. Together, 63% of the computational structures represent the designed order of interactions in which the central NDI2•DAN3 interaction is maintained, while frustration of the NDI1•NDI2 interaction is relieved and AAN4 provides a new donor-acceptor interaction with NDI.

In sum, the MD simulations are consistent with the experimental NMR and CT data and support the proposed design. The several misfolded states suggest that the linkers between monomers provide a wide range of possible folds and that the energy differences between different stacking interactions are not large enough to drive the equilibrium to a single folded state. This is consistent with findings from dynamic combinatorial libraries of DAN and NDI monomers, in which NDI-NDI stacking was more prevalent than expected. 36,42-44 Taken together, these results suggest a complex energy landscape similar to those in proteins, in which the lowest energy structures change in response to the stimulus (Figure 6).

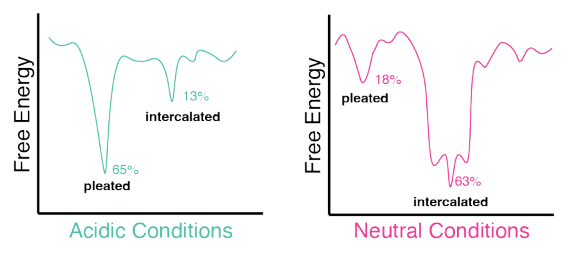


Figure 6. Cartoon energy landscapes for pleated versus intercalated preferences under acidic and neutral conditions.

CONCLUSION

We have designed an abiotic, aqueous supramolecular foldamer, ADAM, that leverages frustration as a design element to promote long-distance structural reorganization when presented with an external stimulus. To our knowledge, we are the first to incorporate strategic frustration into an abiotic scaffold to serve as the source of latent free energy required for re-folding. In agreement with computational studies of stimulus-responsive proteins, our foldamer demonstrates both a stable, optimized core structure, a central DAN-NDI stack, and a frustrated region. Under acidic conditions the frustration arises from the NDI-NDI stack as well as a DAN-AANH+ stack, resulting in a pleated columnar structure. At neutral pH, the interaction between AAN4 and NDI becomes more favorable and provides the opportunity to relieve the NDI1•NDI2 frustration via intercalative folding. Due to the relatively long linkers in our design, three possible pseudo-degenerate stacking arrangements can occur, all involving intercalated stacking in which NDI1 and/or AAN4 fold back to stack in an alternating donor-acceptor-donor-acceptor geometry. The population of more than one folded state under neutral conditions represents another feature of proteins that is rarely mimicked in foldamers - that of conformational dynamics. For example, phosphorylation has been shown to induce structure in an otherwise intrinsically disordered protein that undergoes conformational signaling.⁴ Likewise, protonation of ADAM induces a dominant single fold as compared to the conformational ensemble of folded states at neutral pH.

The ADAM foldamer occupies a unique space in the body of literature surrounding switchable foldamers. While there are examples of long-distance communication resulting in a change of chirality or tautomeric state, ^{12,13,25} the ADAM system demonstrates a novel form of long-distance communication through the NCN in which a stimulus input at the C-terminus results in reorganization of the N-terminus residues while maintaining the central core interaction in aqueous solution. In summary, the ability to harness biological mechanisms such as frustration in abiotic foldamers opens the possibility for increased complexity in synthetic responsive systems.

ASSOCIATED CONTENT

Supporting Information

The Supporting Information is available free of charge on the ACS Publications website.

Synthetic procedures, characterization, NMR and UV-Vis spectra, MD simulation methods (PDF)

AUTHOR INFORMATION

Corresponding Author

Marcey L. Waters – Glen H. Elder, Jr., Distinguished Professor, Department of Chemistry, CB 3290, UNC Chapel Hill, Chapel Hill, NC 27599 USA

ORCID ID: 0000-0002-4917-5755

Email: mlwaters@email.unc.edu

Authors

Hanne C. Henriksen - Department of Chemistry, CB 3290, UNC Chapel Hill, Chapel Hill, NC 27599 USA ORCID ID: 0009-0006-4238-3670

Adam J. Sowers - Department of Chemistry, CB 3290, UNC Chapel Hill, Chapel Hill, NC 27599 USA ORCID ID: 0009-0001-9324-595X

Christopher R. Travis - Department of Chemistry, CB 3290, UNC Chapel Hill, Chapel Hill, NC 27599 USA ORCID ID: 0000-0003-0673-6978

Troy D. Vulpis - Department of Chemistry, CB 3290, UNC Chapel Hill, Chapel Hill, NC 27599 USA ORCID ID: 0000-0002-6407-7133

Thomas A. Cope - Department of Chemistry, CB 3290, UNC Chapel Hill, Chapel Hill, NC 27599 USA ORCID ID: 0009-0000-4579-5861

Sarah K. Ouslander - Department of Chemistry, CB 3290, UNC Chapel Hill, Chapel Hill, NC 27599 USA ORCID ID: 0009-0003-3579-7152

Alexander F. Russell - Department of Chemistry, CB 3290, UNC Chapel Hill, Chapel Hill, NC 27599 USA ORCID ID: 0009-0006-2995-9276

Vojislava Pophristic - Department of Chemistry and Biochemistry, Rowan University, Glassboro, NJ 08028-1701 USA

ORCID ID: 0000-0002-8848-2651

Zhiwei Liu - Department of Chemistry and Biochemistry, Rowan University, Glassboro, NJ 08028-1701 USA

ORCID ID: 0000-0003-1020-7948

ACKNOWLEDGMENT

This work was supported in part by a grant from the NSF CHE-2107685 to M.L.W. This work was supported in part by the National Institute of General Medical Sciences of the National Institutes of Health under award number R01GM110017 to M.L.W. and M. R.G. This work was supported in part by a grant from the NSF CHE-2205220 to V.P. and Z.L. C.R.T. was supported by an NSF GRFP. We thank Dr. Andrew Camp and Dr. Marc ter Horst in the UNC Department of Chemistry NMR Core Laboratory for assistance with NMR analysis on instrumentation acquired through the NSF MRI program under Award No. CHE-1828183. We thank the UNC Department of Chemistry Mass Spectrometry Core Laboratory for their assistance with mass spectrometry analysis on instrumentation supported by the NSF under Grant No. CHE-1726291. We thank Dr. Stu Parnham in the UNC Biomolecular NMR core for assistance with NMR analysis on instrumentation acquired with support from the National Cancer Institute of the National Institutes of Health under award number P30CA016086. Finally, we thank Dr. Abigail Knight for use of her UV-Vis spectrometer.

ABBREVIATIONS

NCN, noncovalent network; NCI, noncovalent interaction; AAN, aminoalkoxy naphthalene; DAN, dialkoxynaphthalene; NDI, naphthalenediimide; ADAM, adaptive donor-acceptor motif; CT, charge transfer.

REFERENCES

- Guo, J.; Zhou, H. X. Protein Allostery and Conformational Dynamics. Chem. Rev. 2016, 116 (11), 6503–6515. https://doi.org/10.1021/acs.chemrev.5b00590.
- (2) Nussinov, R.; Tsai, C. J.; Ma, B. The Underappreciated Role of Allostery in the Cellular Network. *Annu. Rev. Biophys.* 2013, 42
 (1), 169–189. https://doi.org/10.1146/annurev-biophys-083012-130257
- (3) Sol, A.; Tsai, C.; Ma, B.; Nussinov, R. The Origin of Allosteric Functional Modulation: Multiple Pre-Existing Pathways. *Structure* **2009**, *17* (8), 1042–1050. https://doi.org/10.1016/j.str.2009.06.008.
- (4) Tompa, P. The Principle of Conformational Signaling. *Chem. Soc. Rev.* **2016**, 45 (15), 4252–4284. https://doi.org/10.1039/c6cs00011h.
- (5) Schlessinger, J. Cell Signaling by Receptor Tyrosine Kinases. Cell 2000, 103, 211–225. https://doi.org/10.1007/978-90-481-2642-2 16.
- (6) Weis, W. I.; Kobilka, B. K. The Molecular Basis of G Protein-Coupled Receptor Activation. *Annu. Rev. Biochem.* 2018, 87, 897–919. https://doi.org/10.1146/annurev-biochem-060614-033910.
- (7) Ferreiro, D. U.; Hegler, J. A.; Komives, E. A.; Wolynes, P. G. On the Role of Frustration in the Energy Landscapes of Allosteric Proteins. *Proc. Natl. Acad. Sci. U. S. A.* 2011, 108 (9), 3499– 3503. https://doi.org/10.1073/pnas.1018980108.
- (8) Gianni, S.; Freiberger, M. I.; Jemth, P.; Ferreiro, D. U.; Wolynes, P. G.; Fuxreiter, M. Fuzziness and Frustration in the Energy Landscape of Protein Folding, Function, and Assembly. Acc. Chem. Res. 2021, 54 (5), 1251–1259. https://doi.org/10.1021/acs.accounts.0c00813.
- (9) Bryngelson, J. D.; Onuchic, J. N.; Socci, N. D.; Wolynes, P. G. Funnels, Pathways, and the Energy Landscape of Protein Folding: A Synthesis. *Proteins Struct. Funct. Bioinforma.* 1995, 21 (3),

- 167-195. https://doi.org/10.1002/prot.340210302.
- (10) Ferreiro, D. U.; Komives, E. A.; Wolynes, P. G. Frustration, Function and Folding. Curr. Opin. Struct. Biol. 2018, 48, 68–73. https://doi.org/10.1016/j.sbi.2017.09.006.
- (11) Ferreiro, D. U.; Komives, E. A.; Wolynes, P. G. Frustration in Biomolecules. *Q. Rev. Biophys.* **2014**, *47* (4), 285–363. https://doi.org/10.1017/S0033583514000092.
- Brown, R. A.; Diemer, V.; Webb, S. J.; Clayden, J. End-to-End Conformational Communication through a Synthetic Purinergic Receptor by Ligand-Induced Helicity Switching. *Nat. Chem.* 2013, 5 (10), 853–860. https://doi.org/10.1038/nchem.1747.
- (13) Tilly, D. P.; Heeb, J. P.; Webb, S. J.; Clayden, J. Switching Imidazole Reactivity by Dynamic Control of Tautomer State in an Allosteric Foldamer. *Nat. Commun.* **2023**, *14* (1), 8–14. https://doi.org/10.1038/s41467-023-38339-2.
- (14) Mateus, P.; Chandramouli, N.; Mackereth, C. D.; Kauffmann, B.; Ferrand, Y.; Huc, I. Allosteric Recognition of Homomeric and Heteromeric Pairs of Monosaccharides by a Foldamer Capsule. Angew. Chemie - Int. Ed. 2020, 59 (14), 5797–5805. https://doi.org/10.1002/anie.201914929.
- (15) Parks, F. C.; Liu, Y.; Debnath, S.; Stutsman, S. R.; Raghavachari, K.; Flood, A. H. Allosteric Control of Photofoldamers for Selecting between Anion Regulation and Double-to-Single Helix Switching. J. Am. Chem. Soc. 2018, 140 (50), 17711–17723. https://doi.org/10.1021/jacs.8b10538.
- (16) Nelson, J. C.; Saven, J. G.; Moore, J. S.; Wolynes, P. G. Solvophobically Driven Folding of Nonbiological Oligomers. Science (80-.). 1997, 277 (5333), 1793–1796. https://doi.org/10.1126/science.277.5333.1793.
- (17) Lettieri, R.; Bischetti, M.; Gatto, E.; Palleschi, A.; Ricci, E.; Formaggio, F.; Crisma, M.; Toniolo, C.; Venanzi, M. Looking for the Peptide 2.0(5) -Helix: A Solvent- and Main-Chain Length-Dependent Conformational Switch Probed by Electron Transfer across c(α,α) -Diethylglycine Homo-Oligomers. *Biopolymers* 2013, 100 (1), 51–63. https://doi.org/10.1002/bip.22190.
- Weinig, H. G.; Krauss, R.; Seydack, M.; Bendig, J.; Koert, U. Molecular Signal Transduction by Conformational Transmission: Use of Tetrasubstituted Perhydroanthracenes as Transducers. Chem. A Eur. J. 2001, 7 (10), 2075–2088. https://doi.org/10.1002/1521-3765(20010518)7:10<2075::AID-CHEM2075>3.0.CO;2-1.
- (19) Khan, A.; Kaiser, C.; Hecht, S. Prototype of a Photoswitchable Foldamer. Angew. Chemie - Int. Ed. 2006, 45 (12), 1878–1881. https://doi.org/10.1002/anie.200503849.
- (20) Mazzier, D.; Crisma, M.; De Poli, M.; Marafon, G.; Peggion, C.; Clayden, J.; Moretto, A. Helical Foldamers Incorporating Photoswitchable Residues for Light-Mediated Modulation of Conformational Preference. J. Am. Chem. Soc. 2016, 138 (25), 8007–8018. https://doi.org/10.1021/jacs.6b04435.
- (21) Dolain, C.; Maurizot, V.; Huc, I. Protonation-Induced Transition between Two Distinct Helical Conformations of a Synthetic Oligomer via a Linear Intermediate. *Angew. Chemie Int. Ed.* **2003**, 42 (24), 2738–2740. https://doi.org/10.1002/anie.200351080.
- (22) Brioche, J.; Pike, S. J.; Tshepelevitsh, S.; Leito, I.; Morris, G. A.; Webb, S. J.; Clayden, J. Conformational Switching of a Foldamer in a Multicomponent System by PH-Filtered Selection between Competing Noncovalent Interactions. J. Am. Chem. Soc. 2015, 137 (20), 6680–6691. https://doi.org/10.1021/jacs.5b03284.
- (23) LeBailly, B. A. F.; Byrne, L.; Clayden, J. Refoldable Foldamers: Global Conformational Switching by Deletion or Insertion of a Single Hydrogen Bond. *Angew. Chemie Int. Ed.* **2016**, *55* (6), 2132–2136. https://doi.org/10.1002/anie.201510605.
- (24) Peebles, C.; Piland, R.; Iverson, B. L. More than Meets the Eye: Conformational Switching of a Stacked Dialkoxynaphthalene-Naphthalenetetracarboxylic Diimide (DAN-NDI) Foldamer to an NDI-NDI Fibril Aggregate. Chem. - A Eur. J. 2013, 19 (35), 11598–11602. https://doi.org/10.1002/chem.201302009.
- (25) Le Bailly, B. A. F.; Clayden, J. Dynamic Foldamer Chemistry. *Chem. Commun.* 2016, 52 (27), 4852–4863. https://doi.org/10.1039/c6cc00788k.
- (26) Gopalakrishnan, R.; Frolov, A. I.; Knerr, L.; Drury, W. J.; Valeur, E. Therapeutic Potential of Foldamers: From Chemical Biology Tools to Drug Candidates? *J. Med. Chem.* 2016, 59 (21), 9599–9621. https://doi.org/10.1021/acs.jmedchem.6b00376.

- (27) Rinaldi, S. The Diverse World of Foldamers: Endless Possibilities of Self-Assembly. *Molecules* 2020, 25 (14). https://doi.org/10.3390/molecules25143276.
- (28) John, E. A.; Massena, C. J.; Berryman, O. B. Helical Anion Foldamers in Solution. *Chem. Rev.* 2020, 120 (5), 2759–2782. https://doi.org/10.1021/acs.chemrev.9b00583.
- (29) Gellman, S. H. Foldamers: A Manifesto. Acc. Chem. Res. 1998, 31 (4), 173–180.
- (30) Peebles, Cameron; Wight, Christopher D.; Iverson, Brent L.; NDI Foldamers, Assemblies and Conformational Switching. In Naphthalenediimide and Its Congeners: From Molecules to Materials; Pantos, D. G., Ed.; The Royal Society of Chemistry, 2017; pp 72-87. DOI:10.1039/9781782621386-00072.
- (31) Chung, M. K.; White, P. S.; Lee, S. J.; Gagné, M. R.; Waters, M. L. Investigation of a Catenane with a Responsive Noncovalent Network: Mimicking Long-Range Responses in Proteins. *J. Am. Chem. Soc.* **2016**, *138* (40), 13344–13352. https://doi.org/10.1021/jacs.6b07833.
- (32) Iverson, B. L.; Lokey, R. S. Synthetic Molecules That Fold Into a Pleated Secondary Structure In Solution. *Nature* 1995, 375 (6529), 303–305.
- (33) Zych, A. J.; Iverson, B. L. Synthesis and Conformational Characterization of Tethered, Self-Complexing 1,5-Dialkoxynaphthalene/1,4,5,8-Naphthalenetetracarboxylic Diimide Systems. J. Am. Chem. Soc. 2000, 122 (37), 8898–8909. https://doi.org/10.1021/ja0019225.
- (34) Ikkanda, B. A.; Iverson, B. L. Exploiting the Interactions of Aromatic Units for Folding and Assembly in Aqueous Environments. *Chem. Commun.* **2016**, *52* (50), 7752–7759. https://doi.org/10.1039/c6cc01861k.
- (35) Gabriel, G. J.; Sorey, S.; Iverson, B. L. Altering the Folding Patterns of Naphthyl Trimers. J. Am. Chem. Soc. 2005, 127 (8), 2637–2640. https://doi.org/10.1021/ja046722y.
- (36) Cougnon, F. B. L.; Au-Yeung, H. Y.; Pantos, G. D.; Sanders, J. K. M. Exploring the Formation Pathways of Donor-Acceptor Catenanes in Aqueous Dynamic Combinatorial Libraries. *J. Am. Chem. Soc.* 2011, 133 (9), 3198–3207. https://doi.org/10.1021/ja111407m.
- (37) Cubberley, M. S.; Iverson, B. L. 1H NMR Investigation of Solvent Effects in Aromatic Stacking Interactions. *J. Am. Chem. Soc.* **2001**, *123* (31), 7560–7563. https://doi.org/10.1021/ja015817m.
- (38) Freiberger, M. I.; Wolynes, P. G.; Ferreiro, D. U.; Fuxreiter, M. Frustration in Fuzzy Protein Complexes Leads to Interaction Versatility. J. Phys. Chem. B 2021, 125 (10), 2513–2520. https://doi.org/10.1021/acs.jpcb.0c11068.
- (39) Wei, G.; Xi, W.; Nussinov, R.; Ma, B. Protein Ensembles: How Does Nature Harness Thermodynamic Fluctuations for Life? The Diverse Functional Roles of Conformational Ensembles in the Cell. *Chem. Rev.* 2016, 116 (11), 6516–6551. https://doi.org/10.1021/acs.chemrev.5b00562.
- (40) Serjeant, E. P. Zwitterion Ratios of Aminobenzoic Acids. *Aust. J. Chem.* **1969**, *22*, 1189–1192.
- (41) Dupradeau, F. Y.; Pigache, A.; Zaffran, T.; Savineau, C.; Lelong, R.; Grivel, N.; Lelong, D.; Rosanski, W.; Cieplak, P. The R.E.D. Tools: Advances in RESP and ESP Charge Derivation and Force Field Library Building. *Phys. Chem. Chem. Phys.* 2010, 12 (28), 7821–7839. https://doi.org/10.1039/c0cp00111b.
- (42) Cougnon, F. B. L.; Ponnuswamy, N.; Jenkins, N. A.; Pantos, G. D.; Sanders, J. K. M. Structural Parameters Governing the Dynamic Combinatorial Synthesis of Catenanes in Water. *J. Am. Chem. Soc.* 2012, 134 (46), 19129–19135. https://doi.org/10.1021/ja3075727.
- (43) Ponnuswamy, N.; Cougnon, F. B. L.; Dan Pantoş, G.; Sanders, J. K. M. Homochiral and Meso Figure Eight Knots and a Solomon Link. J. Am. Chem. Soc. 2014, 136 (23), 8243–8251. https://doi.org/10.1021/ja4125884.
- (44) Au-Yeung, H. Y.; Pantoş, G. D.; Sanders, J. K. M. Amplifying Different [2]Catenanes in an Aqueous Donor-Acceptor Dynamic Combinatorial Library. J. Am. Chem. Soc. 2009, 131 (44), 16030– 16032. https://doi.org/10.1021/ja906634h.

TOC Graphic

